Design and realization of a magnetic-type absorber with a broadened operating frequency band*

Zhou Yong-Jiang(周永江)†, Pang Yong-Qiang(庞永强), and Cheng Hai-Feng(程海峰)

Science and Technology on Advanced Ceramic Fibers and Composites Laboratory, College of Aerospace and Materials Engineering, National University of Defense Technology, Changsha 410073, *China*

(Received 19 April 2012; revised manuscript received 21 June 2012)

In this paper, we present an efficient method to obtain absorbers with broadened operating frequency bands. They are accomplished by using conventional magnetic absorbing materials (MAMs) in the forms of array and mesh structures, which are similar to those in the case of a frequency selective surface. The proposed approach is verified not only by simulations but also by experimental results under the normal incidence at microwave frequencies. Moreover, the wideband absorber is lighter than the conventional magnetic absorber. These results indicate that our proposed absorbing structures can be used for designing good electromagnetic absorbers.

Keywords: magnetic absorbing material, periodic structure, bandwidth

PACS: 52.25.Os, 68.35.bt, 42.25.Bs **DOI:** 10.1088/1674-1056/22/1/015201

1. Introduction

Absorbing materials, which reduce the reflection of incident waves, have been widely studied in the military field since World War II.[1,2] In recent years, there has been an increasing interest in absorbers with emphasis on their applications in solving electromagnetic pollution problems such as electromagnetic interference (EMI) and electromagnetic compatibility (EMC) due to the growing demands of electronic technologies. Owing to their good impedance matching characteristic, magnetic-type absorbing materials (MAMs) including ferrites[3–5] and metal magnetic powders[6–10] generally have wider absorption bandwidths than the other ones, such as carbon-type absorbers,[11–13] and are among the most extensively applied absorbing materials. In practice, MAMs are manufactured into the form of the Dallenbach structure, i.e., the single-layer structure, and they have some disadvantages such as high density and relatively narrow bandwidth, which restrict their further applications. In order to expand the operating bandwidth, multilayer structures are usually used instead of single-layer ones.[13–17] However, this increases the thickness and the weight of the absorber, which are not desirable in applications. Therefore, how to design simultaneously wideband and light weight absorbers is an important issue.

Frequency selective surfaces (FSSs), consisting of periodically arranged elements with arbitrary geometries or their complementary structures having aperture elements, have applications in various areas, including in the design of antenna randomes, filters, and polarizers.[18] Recently, a simple technique of broadening the operating frequency band by FSS incorporation was studied. For instance, one can embed FSSs into absorbing layers to widen the absorption bandwidth in the frequency range of interest.[19–21] In addition, it was also found that FSSs can be used on the top of an absorbing slab to enlarge the absorption bandwidth.[20,21] What is common for all these enhancement techniques is that the broadening of the bandwidth, without increasing the overall thickness, is achieved by the FSS resonance effect.

In this paper, another effective method of expanding the applicable frequency range is proposed. To derive this valuable strategy, both the absorbing property and the impedance matching characteristic of an actual magnetic Dallenbach absorber are investigated firstly. Inspired by the FSS, we design some wideband absorbers based on periodic structures by using the approximate full-wave method combined with the genetic algorithm. Finally, experimental results are presented to demonstrate these wideband absorbers.

2. Foundation consideration and design

An actual magnetic material is considered as a raw material for absorbers, which consists of polymer composites filled with fine magnetic particles. Its relative complex permittivity and permeability in the frequency range of 2–18 GHz measured using a vector network analyzer are illustrated in Figs. 1(a) and 1(b), respectively.

With the given frequency and thickness, the reflection loss (RL) of an absorber can be calculated by using the following well-known equation:

$$\mathrm{RL} = 20\log|(Z_{\mathrm{s}}-1)/(Z_{\mathrm{s}}+1)|, \tag{1}$$

*Project supported by the Aeronautical Science Foundation of China (Grant No. 2011ZF88013).

†Corresponding author. E-mail: paniamer@yahoo.cn

© 2013 Chinese Physical Society and IOP Publishing Ltd

where Z_s is the normalized characteristic impedance of metal-backed absorbing slabs and can be expressed as

$$Z_s = \sqrt{\mu_r/\varepsilon_r}\tanh\{j(2\pi fd/c)\sqrt{\mu_r\varepsilon_r}\}. \quad (2)$$

Here f is the operating frequency; d is the thickness of the absorber; c is the velocity of light; and μ_r and ε_r are the relative complex permeability and permittivity, respectively.

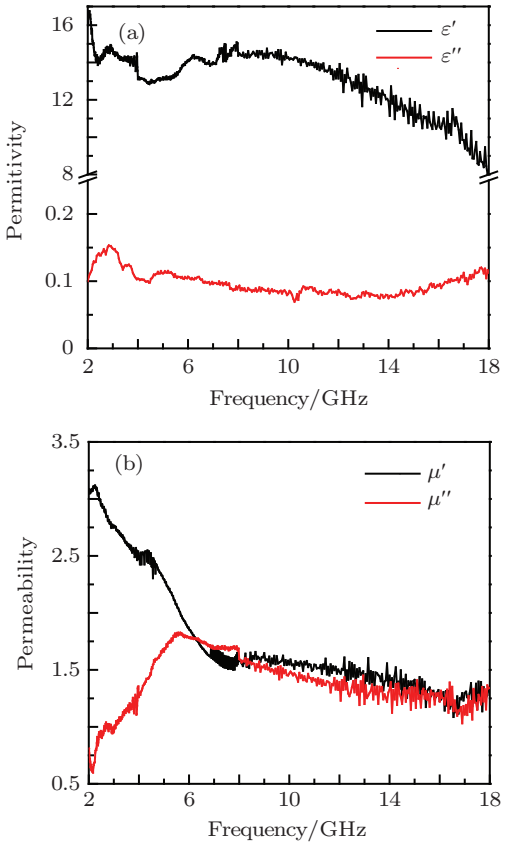


Fig. 1. (color online) Frequency-dependent relative complex (a) permittivity and (b) permeability of the actual magnetic material.

Based on the measured electromagnetic parameters shown in Fig. 1(a), we calculate the absorption properties of the actual MAM with the above equations under the normal incidence. The frequency dependences of RL are shown in Fig. 2(a). It can be observed that the matching frequency f_m tends to shift toward the lower frequency as the thickness of the absorber increases. However, the RL shows narrow-band absorption properties for all cases. Here, the absorption bandwidth is defined as the frequency band in which the RL is less than -10 dB.

To reveal the cause of the narrow-band absorption property clearly, we analyse the impedance matching characteristic of an absorber. Figure 2(b) shows the frequency dependence of the normalized impedance of a 3.0 mm thick absorber. It can be observed that at the matching frequency f_m of 4.0 GHz, the imaginary part of the normalized impedance Z_s is close to zero and the real part approaches to unity, so a lower RL of -19 dB can be obtained at this frequency, which is shown in Fig. 2(a). However, in the frequency range of 4–18 GHz, the absolute value of the imaginary part $|\mathrm{Im}\{Z_s\}|$ is greater than zero, while the real part $\mathrm{Re}\{Z_s\}$ is much smaller than unity, thus leading to the RL enhancement (> -10 dB). In addition, it can also be observed that the imaginary part of Z_s is negative, so that the normalized impedance of the absorber can be rewritten in the lumped-element form as

$$Z_s = R - jX = R + \frac{1}{jC}, \quad (3)$$

where R and C are the equivalent resistance and capacitance, respectively. It should be noted that these equivalent parameters are all functions of the frequency. From the above expression, we can see that $|\mathrm{Im}\{Z_s\}|$ can approach zero by increasing the value of the equivalent capacitance C. From the viewpoint of the impedance matching characteristic, to obtain a lower RL, the equivalent parameter R should be enlarged to be close to unity. Inspired by FSSs, here we propose a way to broaden the absorption bandwidth.

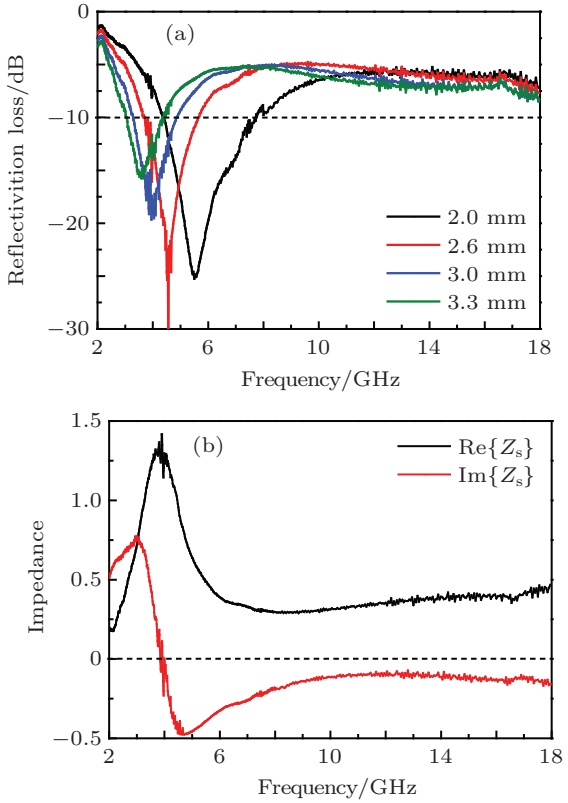


Fig. 2. (color online) Frequency dependences of (a) the reflection losses of absorbers with different thicknesses and (b) the normalized impedance of the absorbing slab with a thickness of 3.0 mm.

Based on the actual material, we firstly present a numerical analysis of some different absorbers with structures similar to those of FSSs. The thicknesses of all these absorbers are assumed to be 3.0 mm. Three cell shapes, i.e., patch, disk, and cross as shown in Fig. 3, are employed to design absorbers with the expanded absorption bandwidths. Here,

we consider two types of periodic structures as in the case of FSSs, namely the array and mesh structures,[18,22] as schematically illustrated with the examples of the patch-shaped unit cell in Fig. 4. Dimension parameters L and D, and periodicity P are determined by using the approximate full-wave method combined with the genetic algorithm for maximizing the −10 dB absorption bandwidth in the frequency range of 2-18 GHz, and the obtained results are summarized in Table 1.

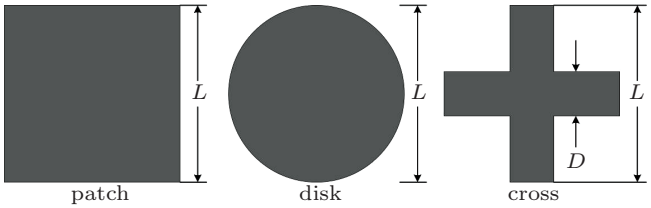


Fig. 3. Element shapes under consideration.

For the first three examples, the actual material is used in the form of the array structure shown in Fig. 4(a). The RLs of the optimized absorbers are plotted in Fig. 5 under the normal incidence in the frequency range of 2–18 GHz. The −10 dB absorption bandwidth of about 4.5–18 GHz can be obtained for these three absorbing materials, while it is only 3.2–5.1 GHz for the original absorber with the same thickness of 3.0 mm, as plotted in Fig. 2(a). This indicates that the operating frequency band of the proposed absorbing structure can be increased remarkably as compared with that of the conventional absorber, as expected.

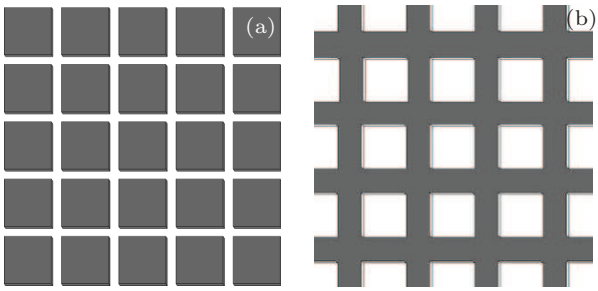


Fig. 4. Proposed absorbing structures with the square patch unit cell: (a) array and (b) mesh. Magnetic material parts are colored grey.

Table 1. Parameters of the optimized absorbers with maximum −10 dB absorption bandwidth.

Unit cell	Array			Mesh		
	P/mm	L/mm	D/mm	P/mm	L/mm	D/mm
Patch	12.4	10.1	–	8.8	6.5	–
Disk	11.0	10.4	–	11.0	10.0	–
Cross	15.8	15.0	7.1	10.0	9.4	1.8

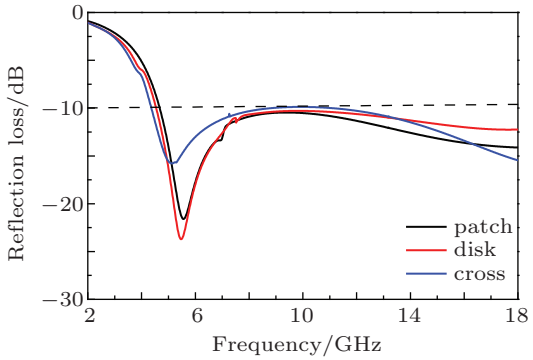


Fig. 5. (color online) Reflection losses of the optimized absorbers of the array structure. Their thicknesses are all 3.0 mm.

With the following three examples we wish to demonstrate that it is also possible to expand the absorption bandwidth by using the conventional lossy materials in the form of the mesh structure illustrated in Fig. 4(b). In Fig. 6, the RLs of optimized absorbers are plotted for the normal incidence, and the thicknesses are also equal to 3.0 mm. Absorption bands of 6.2–18 GHz, 5.6–18 GHz, and 4.6–18 GHz can be achieved for the absorbers consisting of patch, disk, and cross elements, respectively. Some difference of the absorption bandwidth can be observed for these three absorbers, but we can see that the absorption bands are all increased as compared to the reference case in Fig. 2(a), and this is consistent with our earlier intuitive analysis as well.

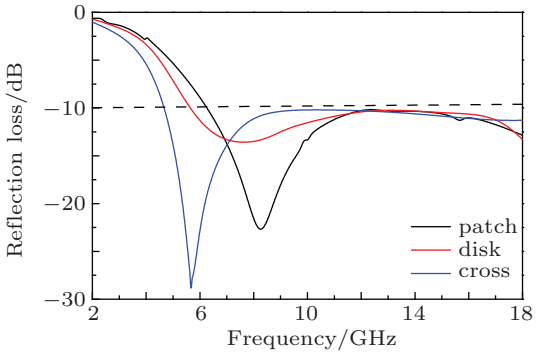


Fig. 6. (color online) Reflection losses of the optimized absorbers consisting of the mesh structure. The thickness is equal to 3.0 mm.

3. Experimental verifications

In this section, we experimentally verify the feasibility of broadening the absorption bandwidths by fabricating conventional absorbing materials in the FSS-like structures. The actual magnetic materials are fabricated into the form of planar slabs with different thicknesses, and then some post-processes are adopted to fabricate experimental samples.

In the first example, the absorber is of the array structure. We choose the square patch as the unit cell for simplfying the fabrication process. We firstly fabricate an actual magnetic planar slab with a thickness of 2.6 mm, and the dielectric material is the polyurethane foam with a relative permittivity of 1.2. Based on these parameters and the measured electromagnetic parameters plotted in Fig. 1, the approximate full-wave method combined with the genetic algorithm is used to optimize parameters P and L to maximize the -10 dB absorption bandwidth. The determined values are $P = 17.3$ mm and $L = 13.4$ mm. The magnetic planar slab is cut into many square patches each with dimensions of 13.4 mm×13.4 mm×2.6 mm, and then inserted into the apertured foam slab. An optical photograph of the fabricated absorber is shown in Fig. 7, and the measured RL in the frequency range of 4–18 GHz compared with the simulated result is plotted in Fig. 8. The great increase of the absorption bandwidth of the fabricated absorber can be easily observed by comparison with the result shown in Fig. 2(a).

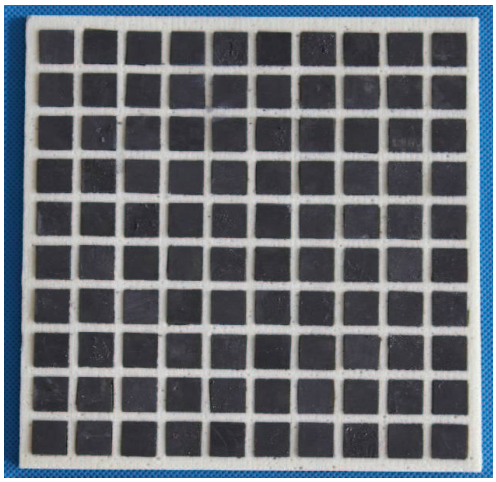


Fig. 7. (color online) Optical photograph of the fabricated absorber with an array structure.

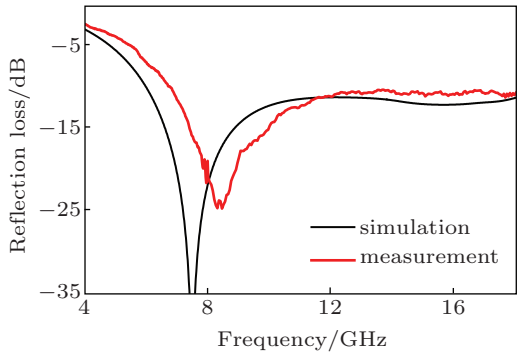


Fig. 8. (color online) Measured reflection loss of the fabricated absorber with an array structure compared with the simulated result.

The fabricated absorber of the mesh structure is similar to the previous one analysed in Section 2. In this example, the disk-shaped aperture element is used for simplfying the fabrication process, and an optical photograph of the fabricated absorber is shown in Fig. 9. Circular holes of the actual magnetic slab are drilled mechanically and then filled with epoxy resin. The relative permittivity of the epoxy resin is approximately equal to 3, and the fabricated magnetic slab is 3.3 mm thick. The structural parameters have the following optimized values: periodicity $P = 14.5$ mm and the diameter of each hole $L = 12.0$ mm. In Fig. 10, we present the measured RL of the fabricated absorber compared with the simulated result. It can be observed that the proposed mesh-structure absorber also shows a broadened operating frequency band. The experimental results, including those in the case of the first sample shown in Fig. 8, are slightly different from the simulations. This is most likely due to fabrication tolerances in the experiment.

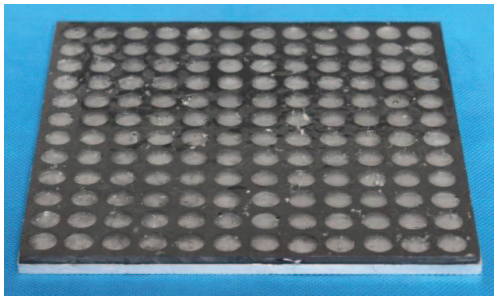


Fig. 9. (color online) Optical photopragh of the fabricated absorber with a mesh structure. The back side of the absorber is an aluminum plate.

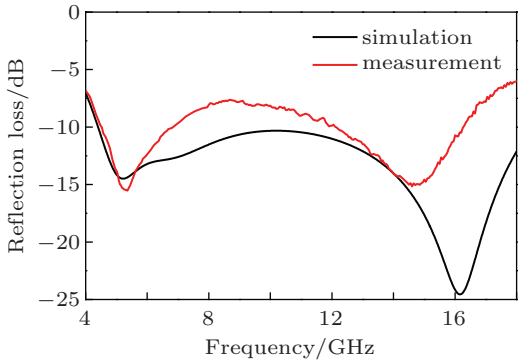


Fig. 10. (color online) Comparison between the measured reflection loss of the fabricated absorber with a mesh structure and the simulated result.

Furthermore, another advantage can be found for our proposed absorbers. That is, the density of our proposed absorbers is smaller than that of the original magnetic slabs, which is beneficial for the practical application. These results indicate that our proposed absorbing structures can be used for designing good electromagnetic absorbers not only with wideband absorption property but also with light weight.

4. Conclusion

Absorbers with broadened operating frequency bandwidths are presented in this paper and demonstrated by the numerical and experimental results. In contrast, the conventional

absorbers with the Dallenbach structure show the narrow-band absorption performance. In addition, the advantage of light weight can be found in our proposed absorbers, which can promote the applications such as electromagnetic shielding, electromagnetic compatibility, and radar cross section reduction. So our proposed absorbing structures can be used in the design of good electromagnetic absorbing materials.

References

[1] Salisbury W W (U.S. Patent) 2 599 944 [1952-6-10]

[2] Knott E F, Shaeffer J F and Tuley M T 2004 *Radar Cross Section* (2nd edn.) (London: Atech House)

[3] Kim D Y, Chung Y C, Kang T W and Kim H C 1996 *IEEE Tran. Magn.* **32** 555

[4] Moucka R, Vilcakova J, Kazantseva N E, Lopatin A V and Saha P 2008 *J. Appl. Phys.* **104** 103718

[5] Kim S S 2011 *IEEE Tran. Magn.* **47** 4314

[6] Liu X G, Geng D Y, Ma S, Meng H, Tong M, Kang D J and Zhang Z D 2008 *J. Appl. Phys.* **104** 064319

[7] Lian L X, Deng L J, Han M, Tang W and Feng S D 2007 *J. Appl. Phys.* **101** 09M520

[8] Liu J R, Itoh M, Terada M, Horikawa T and Machida K 2007 *Appl. Phys. Lett.* **91** 093101

[9] Dong X L, Zhang X F and Zuo F 2008 *Appl. Phys. Lett.* **92** 013127

[10] Zhang B S, Feng Y, Xiong J, Zhang Y and Lu H X 2006 *IEEE Tran. Magn.* **42** 1778

[11] Lee S E, Choi O and Hahn H T 2008 *J. Appl. Phys.* **104** 033705

[12] Wen B, Zhao J J, Duan Y P, Zhang X G, Zhao Y B, Dong C, Liu S H and Li T J 2006 *J. Phys.* D: *Appl. Phys.* **39** 1960

[13] Rosa I M D, Mancinelli R, Sarasini F, Sarto M S and Tamburrano A 2009 *IEEE Tran. Electromagn.Compat.* **51** 700

[14] He Y F, Gong R Z, Nie Y, He H H and Zhao Z S 2005 *J. Appl. Phys.* **98** 084903

[15] Han M G, Ou Y and Deng L J 2009 *J. Magn. Magn. Mater.* **321** 1125

[16] Chamaani S, Mirtaheri S A, Teshnehlab M, Shoorehdeli M A and Seydi V 2008 *PIER* **79** 353

[17] Asi M J and Dib N I 2010 *PIER* B **26** 101

[18] Munk B A 2000 *Frequency Selective Surfaces*: *Theory and Design* (New York: Wiley)

[19] Kazantsev Y N, Lopatin A V, Kazantseva N E, Shatrov A D, Mal'tsev V P, Vilcakova J and Saha P 2010 *IEEE Tran. Antenn. Propag.* **58** 1227

[20] Chen H Y, Zhang H B and Deng L J 2010 *IEEE Antennas Wireless Propag. Lett.* **9** 899

[21] Sun L K, Cheng H F, Zhou Y J and Wang J 2012 *Chin. Phys.* B **21** 055201

[22] Tretyakov S A 2003 *Analytical Modeling in Applied Electromagnetic* (Norwood: Artech House)